Electronic Supplementary Material (ESI) for Dalton Transactions.

Supplemental Information

Investigation of Ternary Metal Dodecaborides $M_1M_2M_3B_{12}$ (M_1, M_2 and M_3 = Zr, Y, Hf and Gd)

Georgiy Akopov[1], Inwhan Roh[1], Zachary C. Sobell[1], Michael T. Yeung[2], and Richard B. Kaner[1,3,4]*

[1]Department of Chemistry and Biochemistry, University of California, Los Angeles (UCLA), Los Angeles, CA 90095, USA

[2]Department of Chemistry, Northwestern University, Evanston, IL 60208, USA

[3]Department of Materials Science and Engineering, University of California, Los Angeles (UCLA), Los Angeles, CA 90095, USA

[4]California NanoSystems Institute (CNSI), University of California, Los Angeles (UCLA), Los Angeles, CA 90095, USA

* Corresponding author: kaner@chem.ucla.edu

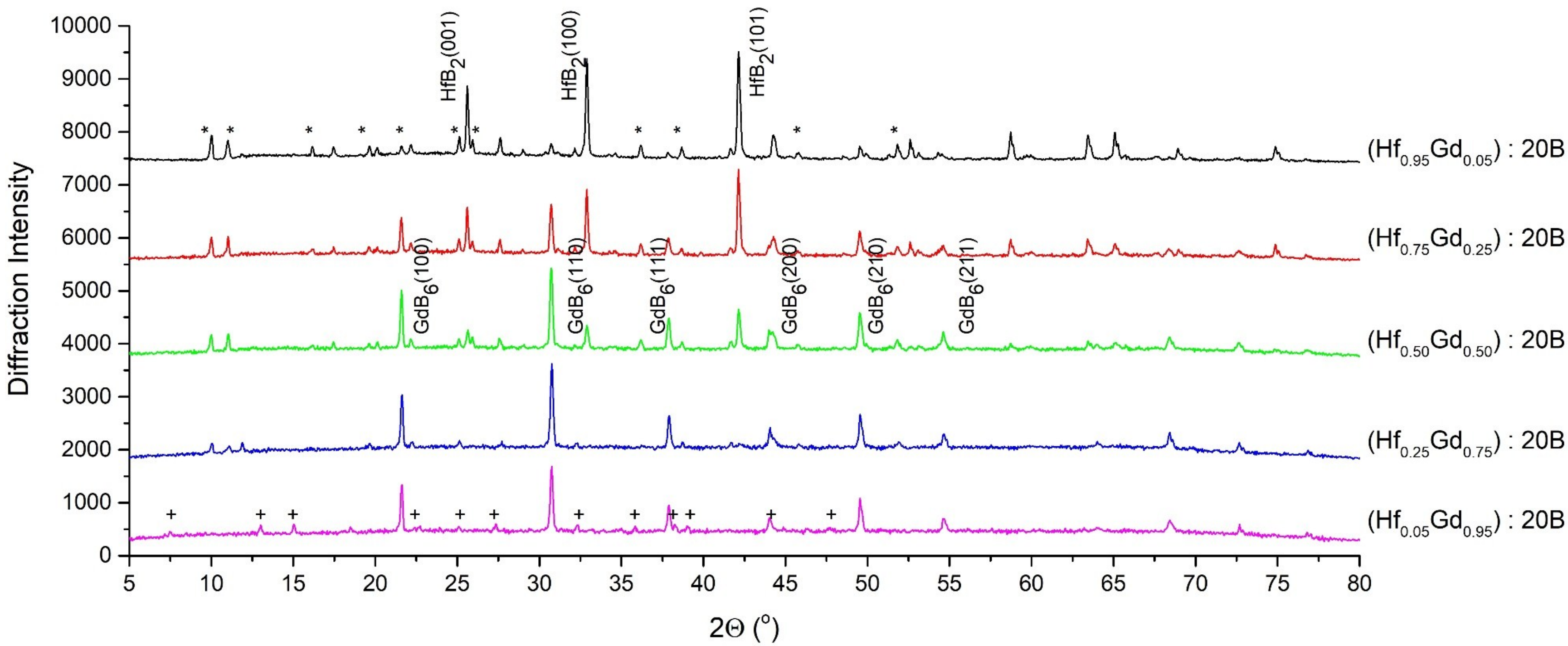

Diffraction Intensity
2Θ (°)
HfB2(001)
HfB2(100)
HfB2(101)
GdB6(100)
GdB6(110)
GdB6(111)
GdB6(200)
GdB6(210)
GdB6(211)
(Hf0.95Gd0.05) : 20B
(Hf0.75Gd0.25) : 20B
(Hf0.50Gd0.50) : 20B
(Hf0.25Gd0.75) : 20B
(Hf0.05Gd0.95) : 20B

(a)

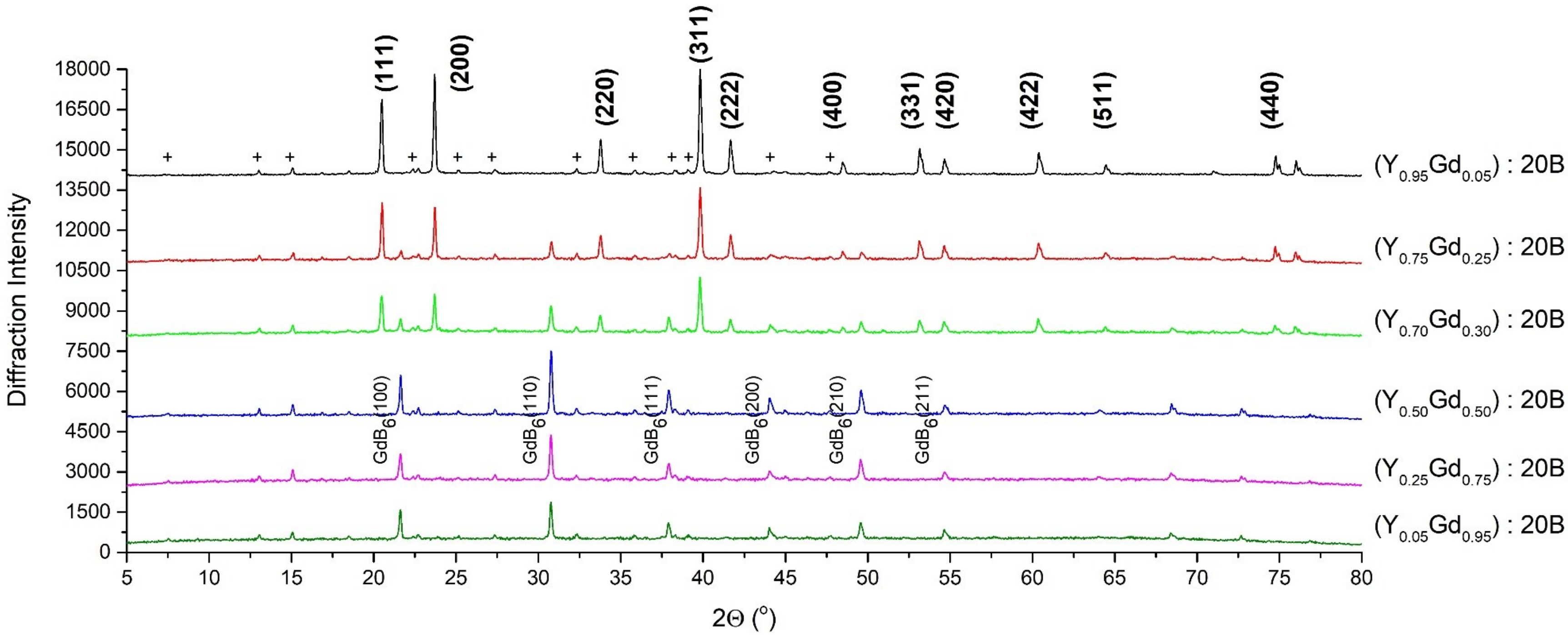

(b)

Figure S1. Powder XRD patterns of: (a) $(Hf_{1-x}Gd_x)$: 20 B, where x = 0.05, 0.25, 0.50, 0.75 and 0.95. The dodecaboride MB_{12} phase does not form for any composition of this alloy. The diboride (HfB_2, P6/mmm, JCPDS 03-065-3387) phase forms at higher concentrations of hafnium, while the hexaboride (GdB_6, $Pm\bar{3}m$, JCPDS 03-065-1826) phase forms for higher concentrations of gadolinium; (b) $(Y_{1-x}Gd_x)$: 20 B, where x = 0.05, 0.25, 0.50, 0.70, 0.75 and 0.95. The dodecaboride MB_{12} phase disappears for compositions of this alloy greater than 30 at.% Gd, with the hexaboride (GdB_6, $Pm\bar{3}m$, JCPDS 03-065-1826) phase forming at higher concentrations of gadolinium. (*) indicates the boron rich phase - solid solution of hafnium in β-rhombohedral boron (HfB_{50}, $R\bar{3}m$, JCPDS 01-086-2400), while (+) indicates GdB_{66} ($Fm\bar{3}c$, JCPDS 00-024-1256).

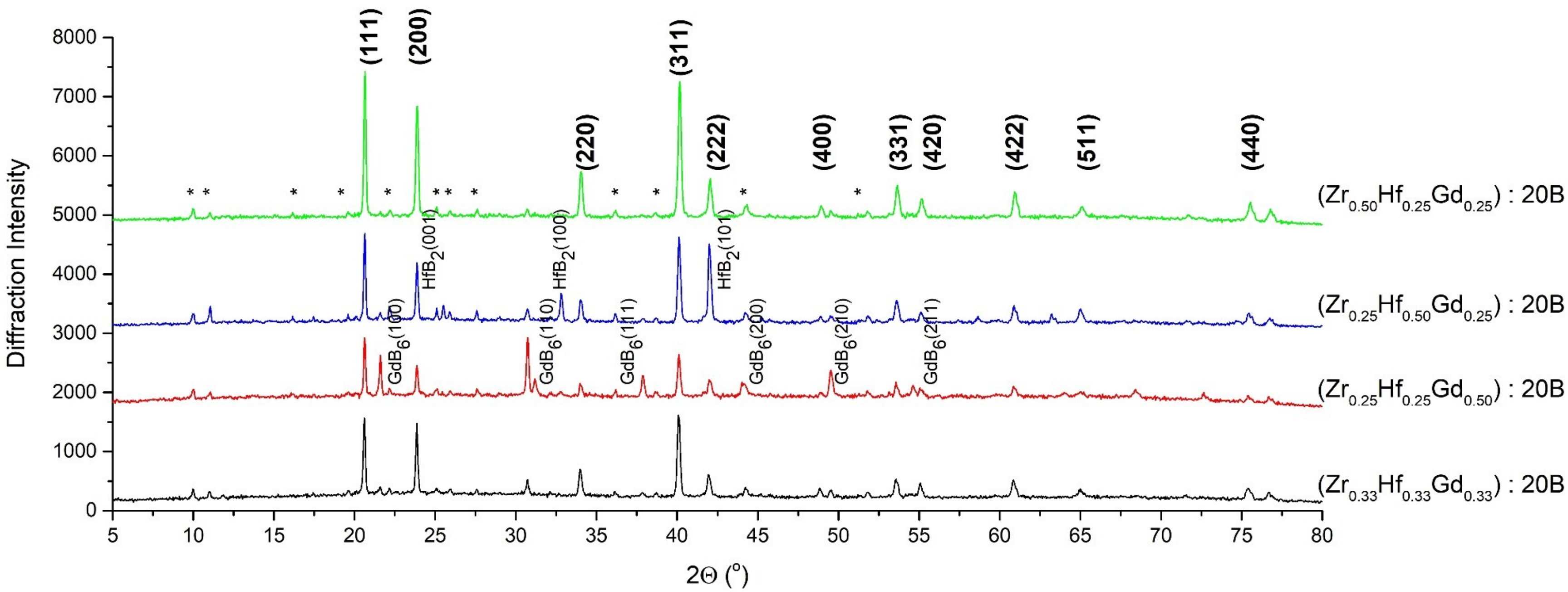

Diffraction Intensity
2Θ (°)
(111)
(200)
(220)
(311)
(222)
(400)
(331)
(420)
(422)
(511)
(440)
HfB2(001)
HfB2(100)
HfB2(101)
GdB6(100)
GdB6(110)
GdB6(111)
GdB6(200)
GdB6(210)
GdB6(211)
(Zr0.50Hf0.25Gd0.25) : 20B
(Zr0.25Hf0.50Gd0.25) : 20B
(Zr0.25Hf0.25Gd0.50) : 20B
(Zr0.33Hf0.33Gd0.33) : 20B

(a)

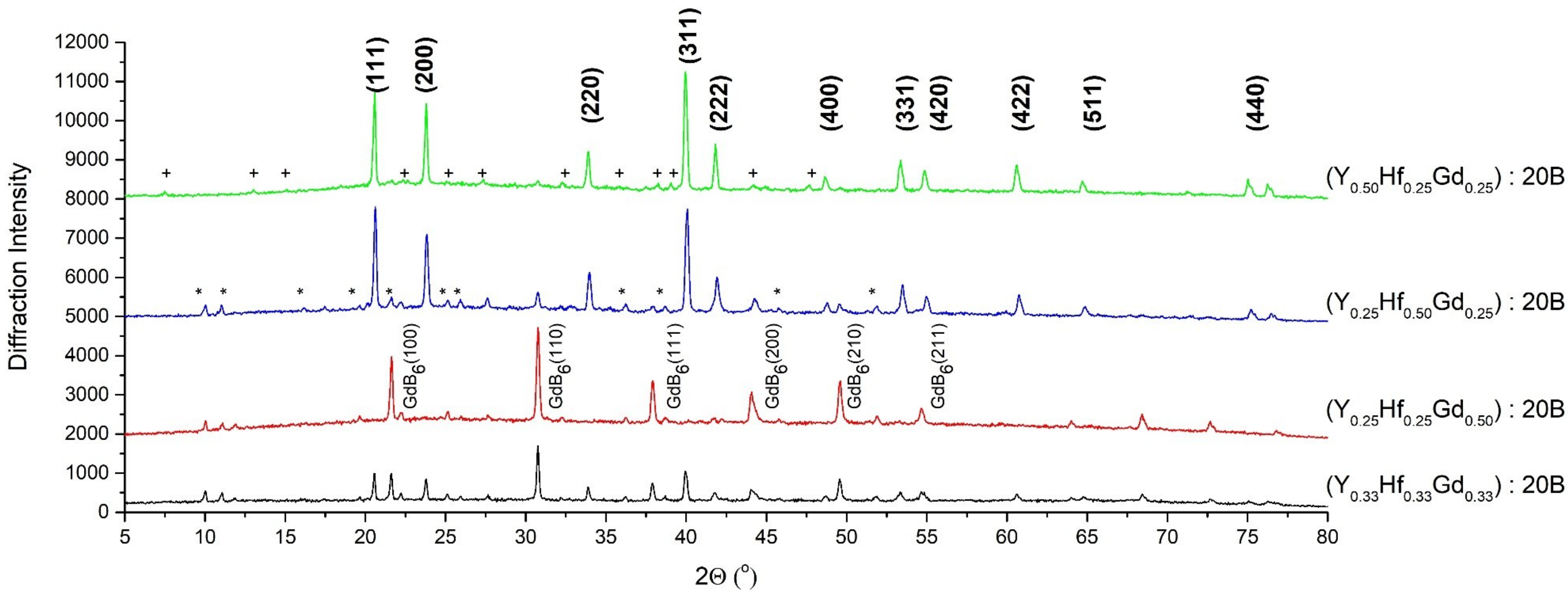

Diffraction Intensity
2Θ (°)
(111)
(200)
(220)
(311)
(222)
(400)
(331)
(420)
(422)
(511)
(440)
GdB6(100)
GdB6(110)
GdB6(111)
GdB6(200)
GdB6(210)
GdB6(211)
(Y0.50Hf0.25Gd0.25) : 20B
(Y0.25Hf0.50Gd0.25) : 20B
(Y0.25Hf0.25Gd0.50) : 20B
(Y0.33Hf0.33Gd0.33) : 20B

(b)

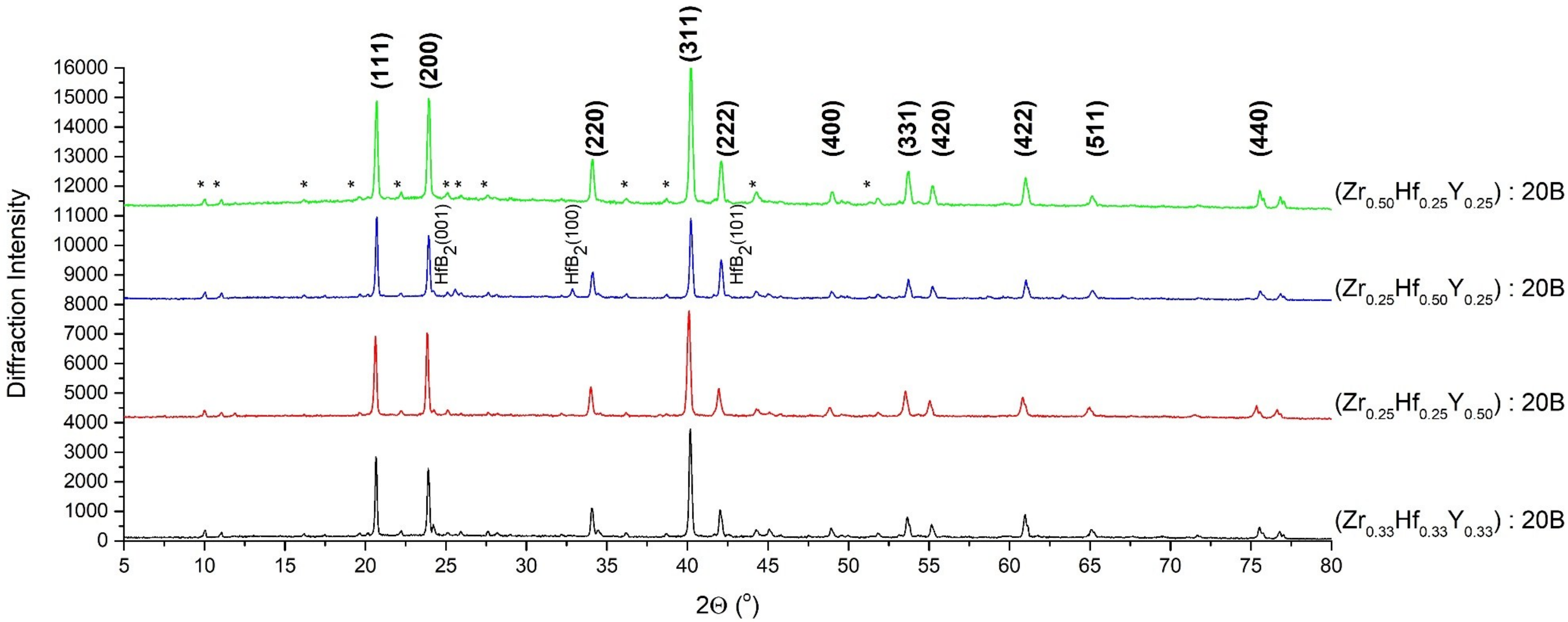
(111)
(200)
(311)
(220)
(222)
(400)
(331)
(420)
(422)
(511)
(440)
HfB2(001)
HfB2(100)
HfB2(101)
Diffraction Intensity
2Θ (°)
(Zr0.50Hf0.25Y0.25) : 20B
(Zr0.25Hf0.50Y0.25) : 20B
(Zr0.25Hf0.25Y0.50) : 20B
(Zr0.33Hf0.33Y0.33) : 20B

(c)

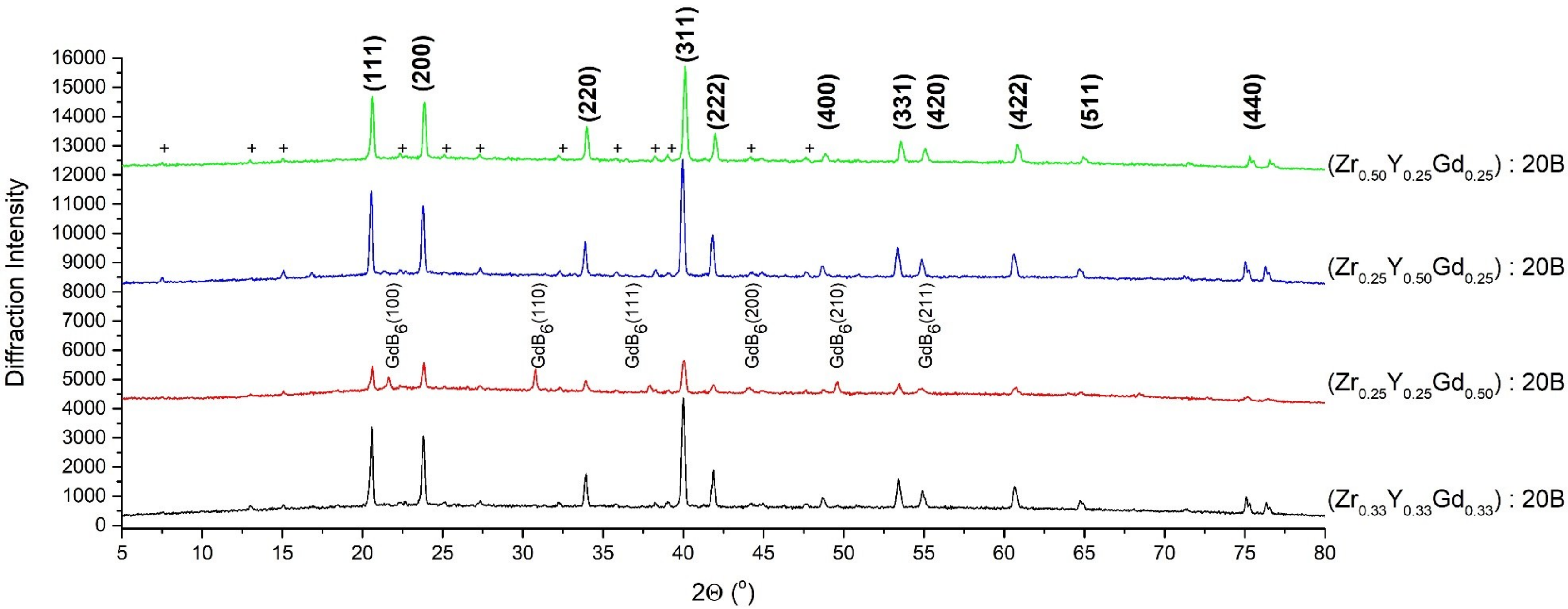

(d)

Figure S2. Powder XRD patterns of: (a) $(Zr_{1-x-z}Hf_xGd_z)$: 20B, where x and z = 0.25, 0.33 and 0.50. The ternary dodecaboride MB_{12} phase can be observed for all 4 compositions, the binary diboride MB_2 phase ($Hf_{1-x}Zr_xB_2$ solid solution) can be observed for $Zr_{0.25}Hf_{0.50}Gd_{0.25}$: 20B, while the hexaboride MB_6 phase (GdB_6) can be observed for all phases except for $Zr_{0.50}Hf_{0.25}Gd_{0.25}$: 20B; (b) $(Y_{1-x-z}Hf_xGd_z)$: 20B, where x and z = 0.25, 0.33 and 0.50. The ternary dodecaboride MB_{12} phase can be observed for all compositions, except for $Y_{0.25}Hf_{0.25}Gd_{0.50}$: 20B, while the binary hexaboride MB_6 phase ($Gd_{1-x}Y_xB_6$ solid solution) can be observed for all compositions except for $Y_{0.50}Hf_{0.25}Gd_{0.25}$: 20B; (c) $(Zr_{1-x-z}Hf_xY_z)$: 20B, where x and z = 0.25, 0.33 and 0.50. The ternary dodecaboride MB_{12} phase can be observed for all 4 compositions, the binary diboride MB_2 phase ($Hf_{1-x}Zr_xB_2$ solid solution) can be observed for $Zr_{0.25}Hf_{0.50}Y_{0.25}$: 20B, while the hexaboride MB_6 phase (YB_6) can be observed for all phases except for $Zr_{0.50}Hf_{0.25}Y_{0.25}$: 20B; (d) $(Zr_{1-x-z}Y_xGd_z)$: 20B, where x and z = 0.25, 0.33 and 0.50. The ternary dodecaboride MB_{12} phase can be observed for all 4 compositions, the binary hexaboride MB_6 phase ($Gd_{1-x}Y_xB_6$ solid solution) can be observed for $Zr_{0.25}Y_{0.25}Gd_{0.50}$: 20B. For all cases: (*) indicates the boron rich phase - solid solution of hafnium-zirconium in β-rhombohedral boron ($Hf_{1-x}Zr_xB_{50}$), both $R\bar{3}m$, JCPDS 01-086-2400 and 03-065-2184, respectively); while (+) indicates GdB_{66} and YB_{66} or their solid solutions (both $Fm\bar{3}c$, JCPDS 00-024-1256 and 01-073-0759, respectively). The peaks were assigned using: HfB_2, *P6/mmm*, JCPDS 03-065-3387, GdB_6, $Pm\bar{3}m$, JCPDS 03-065-1826 and ZrB_{12}, $Fm\bar{3}m$, JCPDS 03-065-3100.

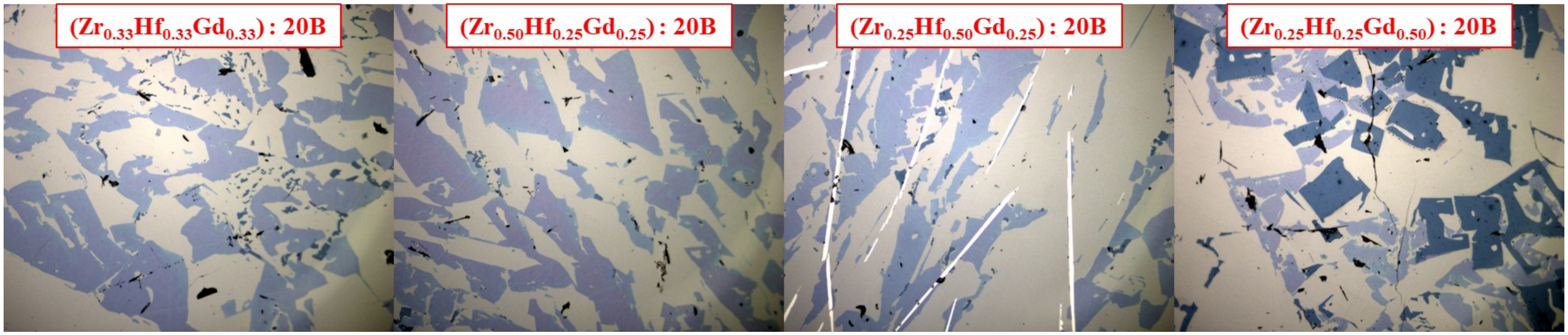
$(Zr_{0.33}Hf_{0.33}Gd_{0.33})$: 20B
$(Zr_{0.50}Hf_{0.25}Gd_{0.25})$: 20B
$(Zr_{0.25}Hf_{0.50}Gd_{0.25})$: 20B
$(Zr_{0.25}Hf_{0.25}Gd_{0.50})$: 20B

(a)

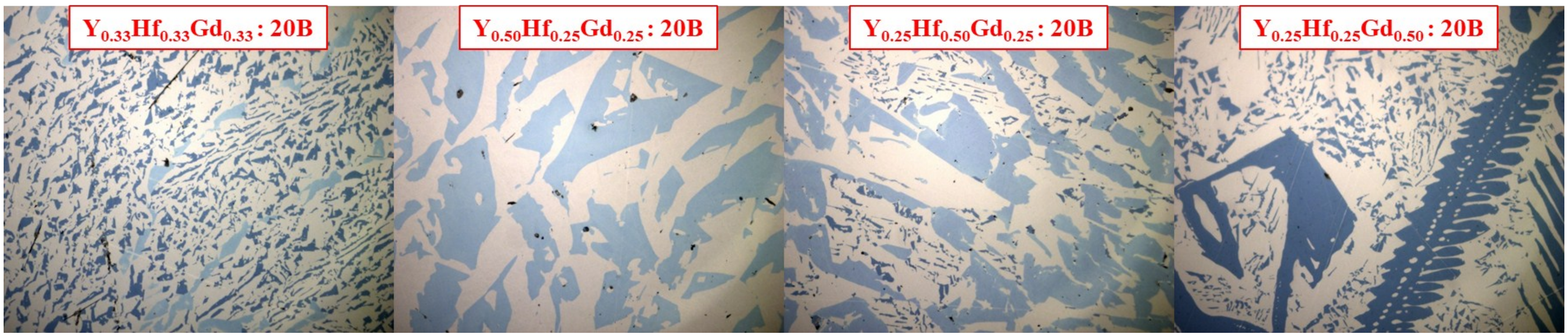
$Y_{0.33}Hf_{0.33}Gd_{0.33}$: 20B
$Y_{0.50}Hf_{0.25}Gd_{0.25}$: 20B
$Y_{0.25}Hf_{0.50}Gd_{0.25}$: 20B
$Y_{0.25}Hf_{0.25}Gd_{0.50}$: 20B

(b)

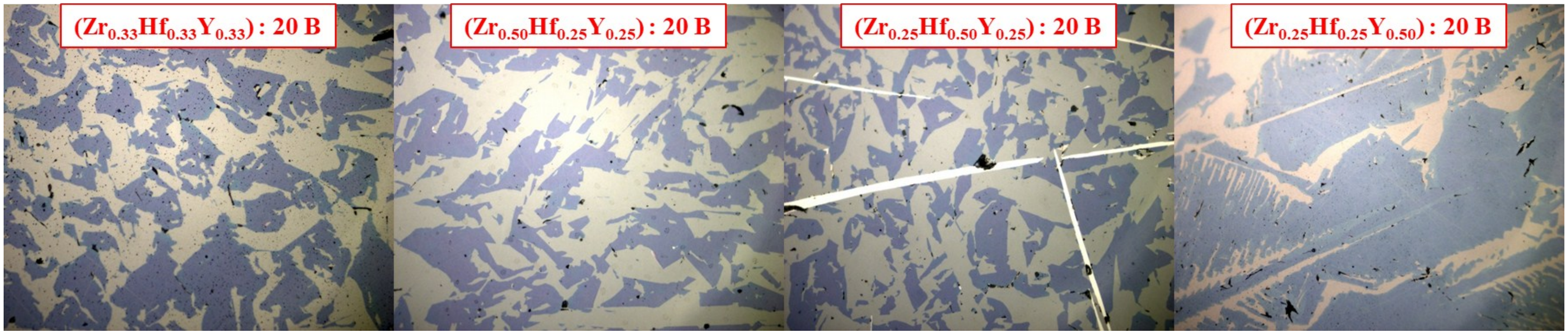

(c)

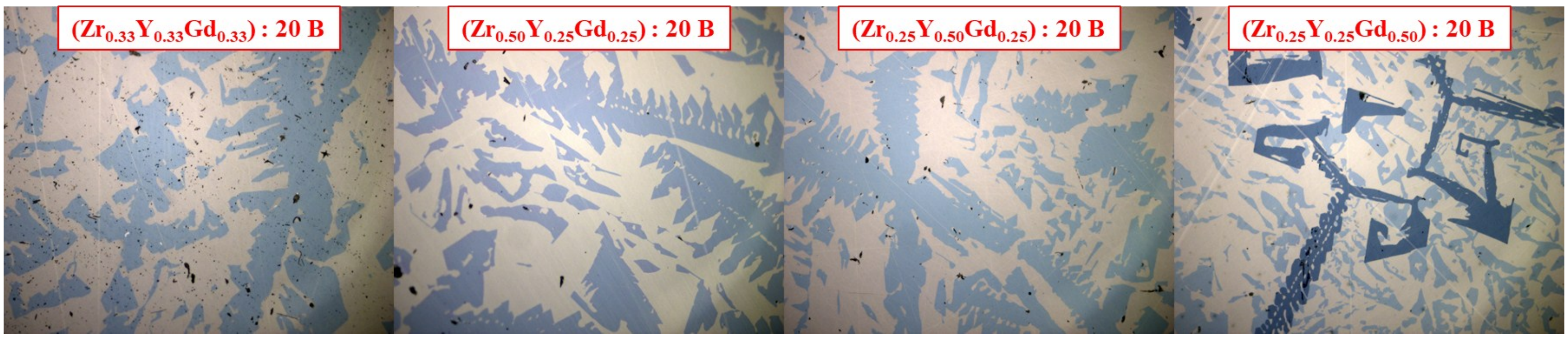

(d)

Figure S3. Optical images of the polished surfaces for: (a) ($Zr_{1-x-z}Hf_xGd_z$) : 20B; (b) ($Y_{1-x-z}Hf_xGd_z$) : 20B; (c) ($Zr_{1-x-z}Hf_xY_z$) : 20B; (d) ($Zr_{1-x-z}Y_xGd_z$) : 20B, where x and z = 0.25, 0.33 and 0.50. In all cases the dodecaboride MB_{12} phases exhibit a color from the blue-violet range, hexaboride MB_6 phases exhibit a deep blue color, diboride phases (white streaks) are colorless, while other areas correspond to the boron rich (also colorless) phases: MB_{50} (for Zr and Hf) and MB_{66} (for Y and Gd). For hexa- and dodecaborides the blue color is due to the metals in +3 oxidation states (Y and Gd), while the violet color is due to the metals in +4 oxidation states (Zr and Hf).